Available online at www.sciencedirect.com

ScienceDirect

Mendeleev Commun., 2019, **29**, 398–399

Mendeleev Communications

Thermal, elastic and optical properties of nanostructured $Pb_{1-x}Ag_xS$ solid solutions

Stanislav I. Sadovnikov

Institute of Solid State Chemistry, Ural Branch of the Russian Academy of Sciences, 620990 Ekaterinburg, Russian Federation. Fax: +7 343 374 4495; e-mail: sadovnikov@ihim.uran.ru

DOI: 10.1016/j.mencom.2019.07.013

For the first time, thermal, elastic and optical properties of limited $Pb_{1-x}Ag_xS$ ($x \leqslant 0.15$) solid solutions have been studied. The replacement of Pb atoms by Ag atoms in nanostructured $Pb_{1-x}Ag_xS$ ($x \leqslant 0.15$) solid solutions with cubic *B*1 structure is accompanied by a decrease in thermal expansion coefficient, a weak increase in elastic moduli and an increase in the band gap width E_g.

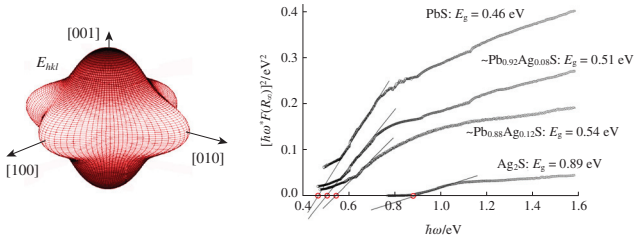

According to published data,[1] the limited solubility of Ag_2S in PbS at 970 K does not exceed 4 mol%, which corresponds to the solid solution $Pb_{0.92}Ag_{0.08}S_{0.96}$. The preparation of $Pb_{1-x}Ag_xS$ solid solution films with $x = 0$–0.16, which are supersaturated at $x > 0.08$, was reported.[2]

Although the PbS and Ag_2S sulfides have been studied in detail,[3–6] there are no data on the thermal expansion and elastic properties of $Pb_{1-x}Ag_xS$ solid solutions, which can be used as solid-phase ion-selective electrodes. In this context, the preparation of lead and silver sulfide solid solutions and their thermal, elastic and optical properties are considered in this work.

Fine PbS, Ag_2S and $Pb_{1-x}Ag_xS$ powders were synthesized by chemical deposition from aqueous solutions of $Pb(AcO)_2$, $AgNO_3$, $Na_3C_6H_5O_7$ (Na_3Cit), NH_4OH and $(NH_2)_2CS$ as described earlier.[2]

According to X-ray diffraction (XRD) data, $Pb_{1-x}Ag_xS$ solid solutions with $x \leqslant 0.12$ are cubic and single-phase, while a $Pb_{0.85}Ag_{0.15}S$ solid solution contains a small impurity of monoclinic silver sulfide along with the main cubic phase. The refinement of XRD patterns showed that the synthesized solid solutions have the formulas ~$Pb_{0.95}Ag_{0.05}S$, ~$Pb_{0.92}Ag_{0.08}S$, ~$Pb_{0.90}Ag_{0.10}S$, ~$Pb_{0.88}Ag_{0.12}S$ and ~$Pb_{0.85}Ag_{0.15}S$. The replacement of Pb^{2+} ions with a radius of 0.120 nm in the PbS lattice by larger Ag^+ ions with a radius of 0.126 nm[7] is accompanied by an increase in the lattice constant a_{B1} of the cubic solid solutions. According to scanning electron microscopy data, the average particle sizes in deposited $Pb_{1-x}Ag_xS$, PbS and Ag_2S powders were about 300–500, 100 and 500 nm, respectively.

Figure 1 shows the temperature dependence of the average linear thermal expansion coefficient $\alpha_{aver}(T)$ of $Pb_{1-x}Ag_xS$ solid solutions, which slightly increased with T in the test temperature range. A larger increase in α_{aver} with temperature was observed in the $Pb_{0.85}Ag_{0.15}S$ solid solution containing an impurity of silver sulfide. The function $\alpha_{aver}(T)$ for $Pb_{1-x}Ag_xS$ can be approximated by the second-order polynomial $\alpha_{aver}(T) = a_0 + a_1T + a_2T^2$. The replacement of lead atoms by silver atoms in solid solutions leads to a small decrease in thermal expansion coefficients (Figure 1), which can be caused by, on the one hand, an increase in the lattice constant and, on the other hand, the reduced anharmonicity of atomic vibrations. Indeed, the lattice constant α_{B1} of $Pb_{1-x}Ag_xS$ rose from 0.5932 to 0.5937 nm with an increase in x from 0 to 0.15. However, this rise of the lattice constant is insufficient for a decrease in $\alpha(300)$ from 20.8×10^{-6} to 18.6×10^{-6} K^{-1}. Hence, it follows that the observed decrease in α of $Pb_{1-x}Ag_xS$ solid solutions with x is caused by a reduction of the anharmonicity of atomic vibrations.

The linear thermal expansion coefficient $\alpha(T)$ is related to the specific heat capacity $C_{sp} = C_V/\nu_m$ per unit volume of substance by the equation

$$\alpha(T) = \frac{\gamma C_{sp}(T)}{3B} \equiv \frac{\gamma}{3B}\frac{C_V(T)}{\nu_m}, \quad (1)$$

where γ is the Grüneisen constant, B is the bulk modulus, and ν_m is the molar volume. The values of γ, C_V and ν_m do not depend almost on $Pb_{1-x}Ag_xS$ composition in narrow region $0 < x < 0.15$. Therefore, it follows from equation (1) that $\alpha(300)$ decreases with x due to a small growth of the bulk modulus $B = (c_{11} + 2c_{12})/3$ (ref. 8) and elastic constants c_{11} and c_{12}.

Earlier,[3] the elastic compliance constants s_{11}, s_{12} and s_{44} of the elasticity tensor for a PbS single crystal of 8.01×10^{-12}, -2.0×10^{-12} and 59.3×10^{-12} m^2 N^{-1}, respectively, at 300 K, were reported. The measured temperature dependences $\alpha(T)$ for $Pb_{1-x}Ag_xS$ solid solutions are similar to $\alpha(T)$ for PbS, and identical cubic structures indicate that PbS and $Pb_{1-x}Ag_xS$ solid solutions have similar temperature dependences of elastic moduli and elastic compliance constants s_{11}, s_{12} and s_{44}, which are 7.69×10^{-12},

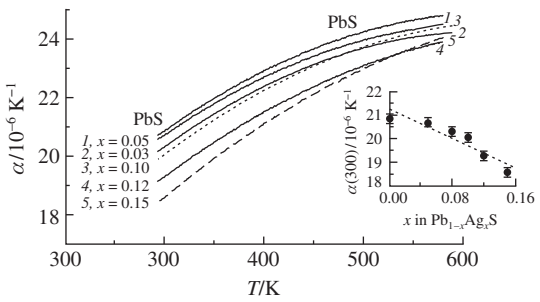

Figure 1 Average thermal expansion coefficients $\alpha_{aver}(T)$ of PbS and $Pb_{1-x}Ag_xS$ solid solutions: (*1*) $Pb_{0.95}Ag_{0.05}S$, (*2*) $Pb_{0.92}Ag_{0.08}S$, (*3*) $Pb_{0.90}Ag_{0.10}S$, (*4*) $Pb_{0.88}Ag_{0.12}S$ and (*5*) $Pb_{0.85}Ag_{0.15}S$. Insert: α_{aver} at 300 K as a function of the composition of solid solutions.

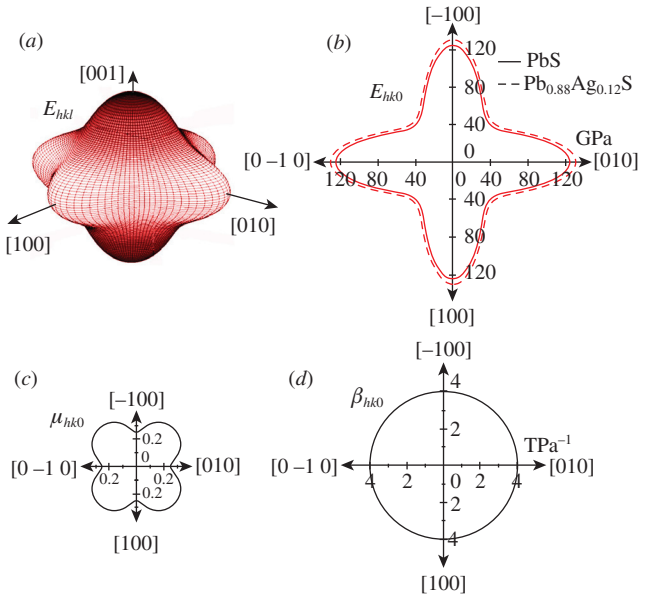

Figure 2 Elastic properties of PbS (solid line) and $Pb_{0.88}Ag_{0.12}S$ (dashed line) as a function of the direction [*hkl*]: (*a*) spatial distribution of elastic modulus E_{hkl} of PbS; (*b*) elastic modulus E_{hkl} distributions for PbS and $Pb_{0.88}Ag_{0.12}S$ in the (*hk*0) plain; (*c*) distributions of Poisson's ratio μ_{hkl}, and (*d*) linear compressibility β_{hkl} in the (*hk*0) plain. Distributions of E_{hkl}, μ_{hkl} and β_{hkl} in planes (*h*0*l*) and (0*kl*) have the same shape.

-1.92×10^{-12}, and 56.7×10^{-12} m^2 N^{-1}, respectively, for the solid solution $Pb_{0.88}Ag_{0.12}S$. Based on s_{11}, s_{12}, and s_{44} for monocrystal particles of PbS and $Pb_{0.88}Ag_{0.12}S$, it is possible to find the elastic modulus E, Poisson's ratio μ, and linear compressibility β as a function of the [*hkl*] directions. According to published data,[9] these functions are

$$E_{hkl} = \frac{1}{s_{11} - 2(s_{11} - s_{12} - 0.5s_{44})\Gamma},$$
$$\mu_{hkl} = \frac{1}{2} - \frac{E_{hkl}(s_{11}^2 + s_{11}s_{12} - 2s_{12}^2)}{2(s_{11} - s_{12})}, \quad (2)$$

where $\Gamma = (h^2k^2 + k^2l^2 + h^2l^2)/(h^2 + k^2 + l^2)^2$.

The calculated dependences of elastic characteristics of monocrystalline PbS and $Pb_{0.88}Ag_{0.12}S$ particles from a direction [*hkl*] are shown in Figure 2. Spatial distribution of the elastic modulus E_{hkl} of lead sulfide [Figure 2(*a*)] is symmetric concerning planes (*hk*0), (*h*0*l*) and (0*kl*). Distributions of elastic modulus E_{hkl} of sulfide PbS and solid solution $Pb_{0.88}Ag_{0.12}S$ in a plane (*hk*0) are shown in Figure 2(*b*). Apparently, the partial replacement of Pb atoms in PbS by Ag atoms leads to a small growth of the elastic modulus E: the maximum and minimum values of E for PbS or

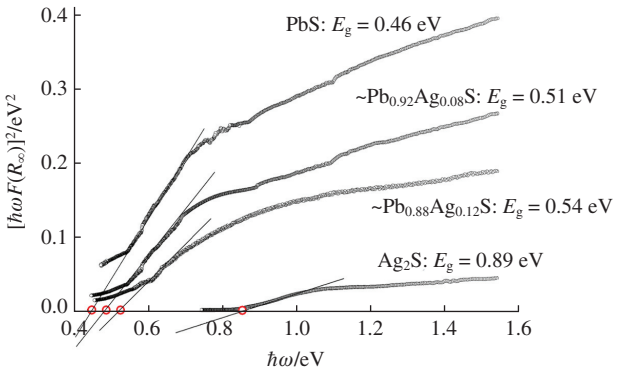

Figure 3 Plots of $[\hbar\omega F(R\infty)]^2$ *vs.* photon energy $\hbar\omega$ and band gaps E_g for the PbS, Ag_2S, $Pb_{0.92}Ag_{0.08}S$ and $Pb_{0.88}Ag_{0.12}S$ fine powders.

$Pb_{0.88}Ag_{0.12}S$ are 124.8 and 56.1 or 128.4 and 58.4 GPa, respectively. Distributions of Poisson's ratio μ_{hkl} and linear compressibility β_{hkl} in a plane (*hk*0) are shown in Figure 2(*c*),(*d*). Partial replacement of Pb atoms by Ag atoms does almost not affect Poisson's ratio μ and the linear compressibility β. The linear compressibility β_{hkl} is 4.01 TPa^{-1} in any direction.

The optical properties of the fine powders of PbS, Ag_2S and $Pb_{1-x}Ag_xS$ were estimated from the reflectance spectra, and the band gaps E_g of sulfide solid solutions and lead and silver sulfides were determined from the reflectance spectra in the $[\hbar\omega F(R_\infty)]^2 \leftrightarrow \hbar\omega$ coordinates (Figure 3). To calculate the band gap energy of the prepared fine sulfide powders, the Kubelka–Munk function[10] was used

$$[\hbar\omega F(R_\infty)]^{1/n} = A(\hbar\omega - E_g), \quad (3)$$

where $\omega = 2\pi c/\lambda$ is the incident light frequency, $\hbar\omega = 2\pi\hbar c/\lambda = \hbar c/\lambda$ is the photon energy, and E_g is the band gap. The function $F(R_\infty) = (1 - R)^2/2R$ was determined from the reflectivity R measured in relative units. For a direct transition, n is 1/2 and the Kubelka–Munk function is transformed to the Tauc relation

$$[\hbar\omega F(R_\infty)]^2 = A(\hbar\omega - E_g). \quad (4)$$

Function (4) is usually used for the quantitative processing of experimental data on optical properties and band gaps. The band gaps E_g of the fine powders of PbS, $Pb_{0.92}Ag_{0.08}S$, $Pb_{0.88}Ag_{0.12}S$ and Ag_2S varied from 0.46 to 0.89 eV. Thus, the replacement of lead with silver in PbS was accompanied by an increase in the band gap E_g.

Thus, the doping of a metal sublattice of lead sulfide by silver and the replacement of Pb atoms by Ag atoms in limited cubic solid solutions $Pb_{1-x}Ag_xS$ ($x \leqslant 0.15$) is accompanied by an insignificant growth of the lattice constant of cubic solid solutions, a decrease in thermal expansion coefficients caused by a reduction of the anharmonicity of atomic vibrations, a weak increase in elastic moduli and a rise of the band gap E_g value from 0.46 to 0.54 eV with a change in x from 0 to 0.12.

The author is grateful to D. A. Yagodin for his assistance in dilatometry measurements. This study was supported by the Russian Science Foundation (grant no. 17-73-10104).

References

1 L. E. Shelimova, V. N. Tomashik and V. I. Grytsiv, *Diagrammy sostoyaniya v poluprovodnikovom materialovedenii, sistemy na osnove khal'kogenidov Si, Ge, Sn, Pb (Phase Diagrams in Semiconductor Materials Science, Systems Based on Si, Ge, Sn and Pb Chalcogenides)*, ed. V. S. Zemskov, Nauka, Moscow, 1991 (in Russian).
2 L. N. Maskaeva, V. F. Markov, T. V. Vinogradova, A. A. Rempel and A. I. Gusev, *Poverkhnost*, 2003, no. 9, 35 (in Russian).
3 S. I. Sadovnikov and A. I. Gusev, *J. Alloys Compd.*, 2014, **610**, 196.
4 S. I. Sadovnikov, A. I. Gusev and A. A. Rempel, *Russ. Chem. Rev.*, 2016, **85**, 731.
5 S. I. Sadovnikov, A. A. Rempel and A. I. Gusev, *Russ. Chem. Rev.*, 2018, **87**, 303.
6 S. V. Rempel, Yu. V. Kuznetsova and A. A. Rempel, *Mendeleev Commun.*, 2018, **28**, 96.
7 R. D. Shannon, *Acta Crystallogr., Sect. A*, 1976, **32**, 751.
8 G. A. Alers, in *Physical Acoustics. Principles and Methods, Lattice Dynamics*, ed. W. P. Mason, Academic Press, New York, 1965, vol. III, part B, ch. 1, pp. 12–56.
9 T. Gnäupel-Herold, P. C. Brand and H. J. Prask, *Adv. X-Ray Anal.*, 1998, **42**, 464.
10 P. Kubelka and F. Munk, *Z. Tech. Phys.*, 1931, 593.

Received: 28th January 2019; Com. 19/5813